Supplementary Information

Photoreactivity of Thiophene-based Core@Shell Nanoparticles: The Effect of Photoinduced Charge Separation on *In Vivo* ROS Production

Mattia Zangoli[a‡], Andrea Cantelli[b‡], Andrea Candini[a], Anna Lewinska[c], Federica Fardella[d], Angela Tino[d], Giuseppina Tommasini[d], Maciej Wnuk[c], Matteo Moschetta[e], Sara Perotto[e], Marco Lucarini[b], Claudia Tortiglione[d], Guglielmo Lanzani[e], Francesca Di Maria[a*]*

[§] Istituto per la Sintesi Organica e Fotoreattività (ISOF), Consiglio Nazionale delle Ricerche, Via Gobetti 101, I-40129 Bologna, Italy

[Ø] Dpt of Chemistry Giacomo Ciamician, University of Bologna, Via Selmi 2, I-40126 Bologna, Italy

[Δ] Istituto di Scienze Applicate e Sistemi Intelligenti "E. Caianiello", Consiglio Nazionale delle Ricerche, Via Campi Flegrei 34, I-80078 Pozzuoli, Italy

[‡]Department of Biotechnology, University of Rzeszow, Pigonia 1, 35-310 Rzeszow, Poland

[¶] Center for Nano Science and Technology @PoliMi, Istituto Italiano di Tecnologia, via Pascoli 70/3, 20133 Milano, Italy.

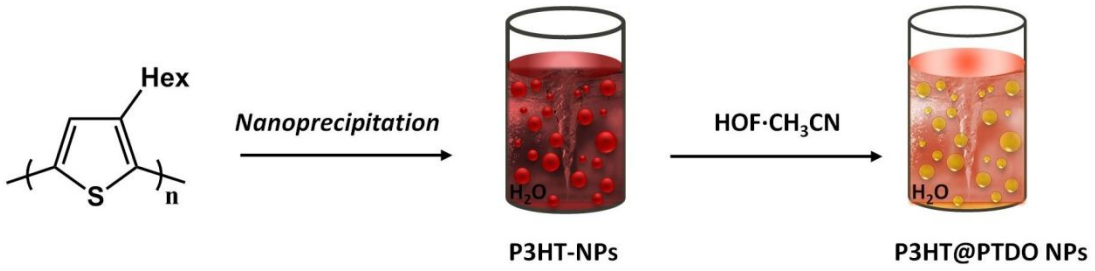

Figure S1. Sketch illustrating the strategy employed for the preparation of P3HT-NPs and P3HT@PTDO NPs.

Nanoparticles	Hydrodynamic diameter (nm)	Z-potential (mV)
P3HT-NPs	380 ± 26	-39.0
P3HT@PTDO$_{0.5}$NPs	390 ± 27	-43.4
P3HT@PTDO$_{1}$NPs	380 ± 28	-48.8
P3HT@PTDO$_{1.5}$NPs	385 ± 26	-52.8

Table S1. Size and Z-potential values of nanoparticles obtained by DLS.

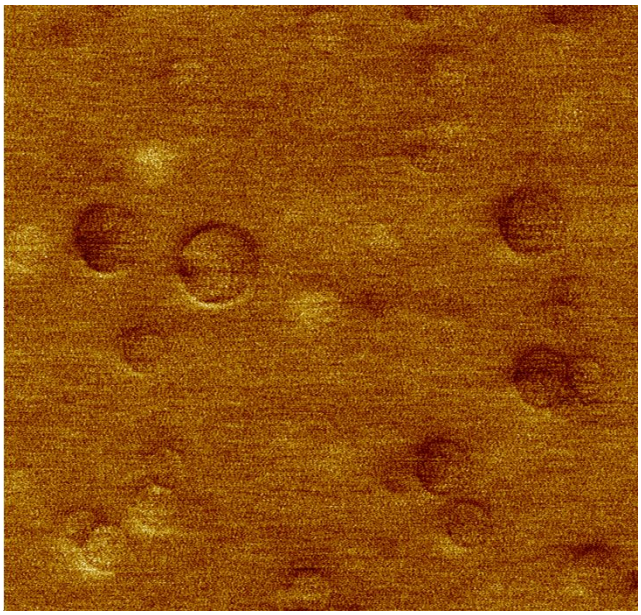

Figure S2. Difference between Figures 1B – 1C. The outer corona present in Figures 1 B and C is absent or displays a dark contrast, indicating that during illumination the SP value of the shell is decreased less than the one of the core. Z-scale: 60 mV. Scale bar: 1 μm.

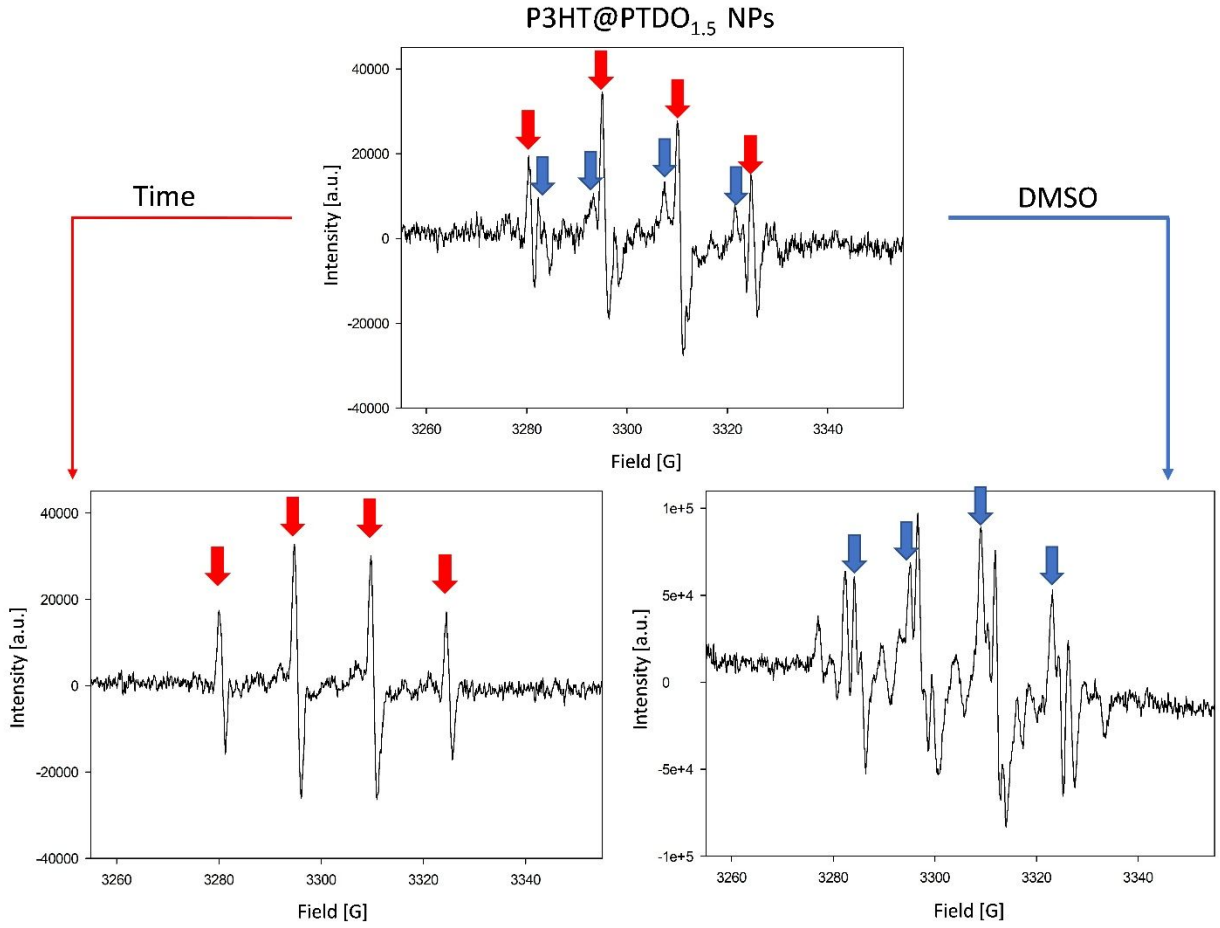

Figure S3. Discrimination of the two radicals trapped by DMPO. On the left, marked in red, the signal of DMPO-OH adduct, isolated by delaying the measurement by a few seconds. On the right, marked in blu, the signals of DMPO-OOH, isolated by adding DMSO to quench the ·OH radical.

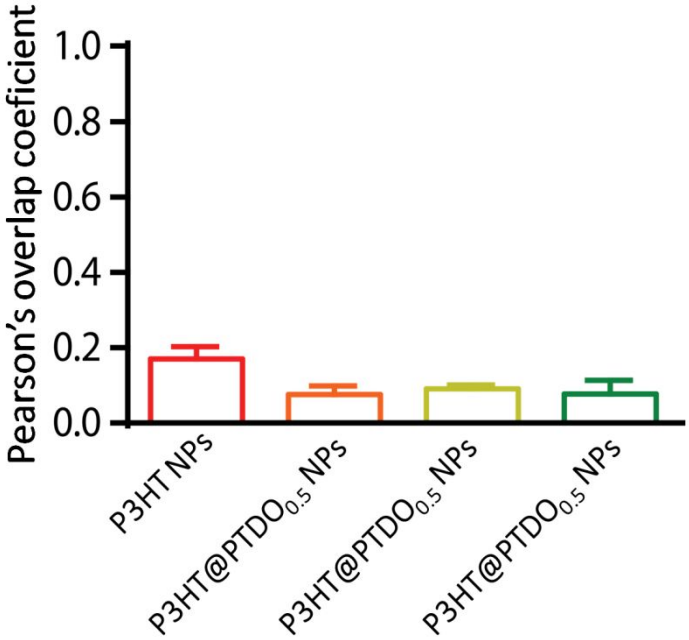

Figure S4. Histograms representing the distribution of the Pearson's correlation coefficient between NPs and CellBright. Co-localization analysis was performed with ImageJ, JACoP plugin. Kruskal-Wallis test with Dunn's correction; n=6, 10, 10 and 6 for P3HT NPs, P3HT@PTDO$_{0.5}$ NPs, P3HT@PTDO$_1$ NPs, and P3HT@PTDO$_{1.5}$ NPs, respectively.

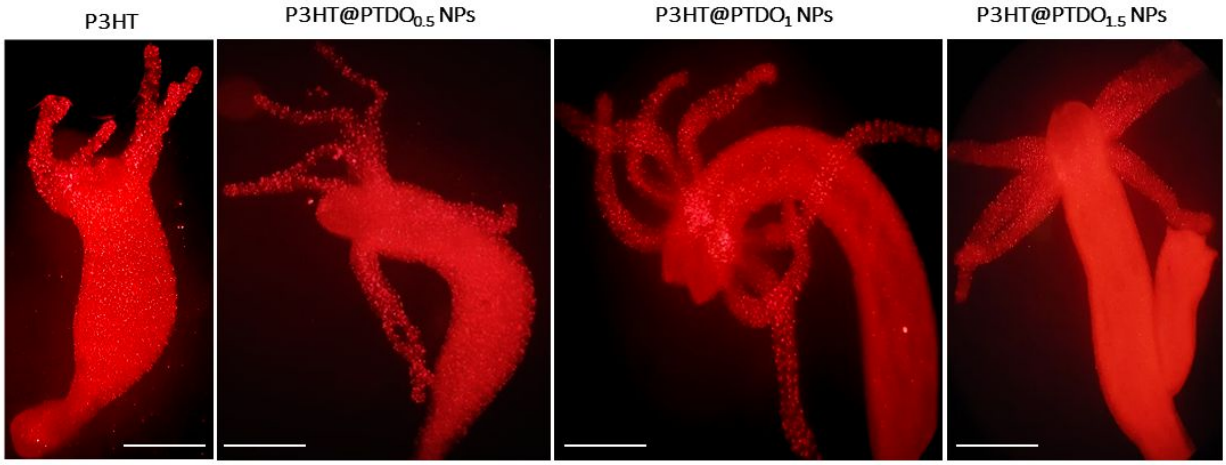

Figure S5. Fluorescence imaging of living *Hydra* polyps treated with P3HT NPs and P3HT@PTDO$_x$ NPs. Scale bars: 500 µm.

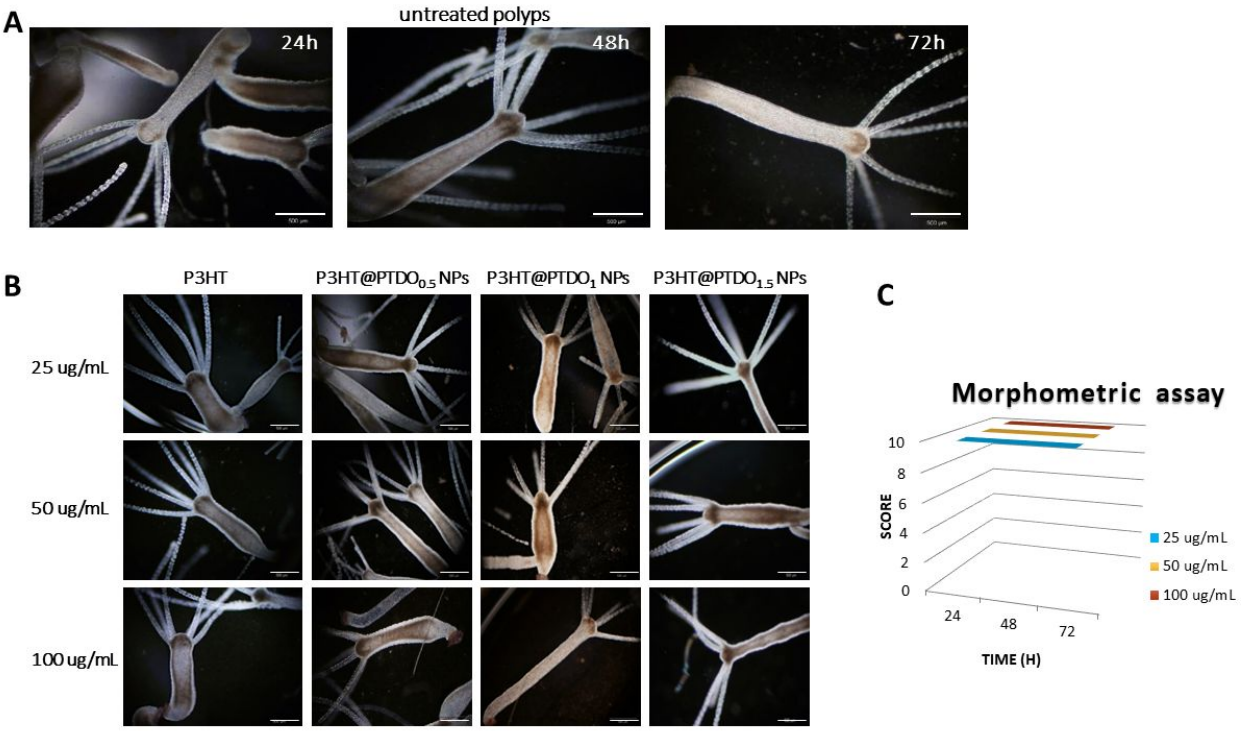

Figure S6. Toxicological evaluation of P3HT NPs and P3HT@PTDO$_x$ NPs on Hydra. A) control polyps morphology; scale bars 500 μm. B) Representative images of polyps exposed to P3HT NPs and P3HT@PTDO$_x$ NPs for 72 h, scale bars 1 mm. C) Dose-response curves showing median morphological scores after 72 h of continuous incubation with P3HT@PTDO$_{1.5}$ NPs as a function of the NPs concentration (n=20). The morphology of animals was not affected by treatment with P3HT NPs and P3HT@PTDO$_x$ NPs, up to 72 h of continuous incubation with 25, 50, 100 μg mL-1, indicating the absence of dose-dependent toxicological effects.